ACS Catalysis

Research Article

pubs.acs.org/acscatalysis

First-Principles Study of Structure Sensitivity of Ethylene Glycol Conversion on Platinum

Xiang-Kui Gu,[†] Bin Liu,[‡] and Jeffrey Greeley*,[†]

[†]School of Chemical Engineering, Purdue University, West Lafayette, Indiana 47907, United States

[‡]Department of Chemical Engineering, Kansas State University, Manhattan, Kansas 66506, United States

Supporting Information

ABSTRACT: Periodic density functional theory (DFT) calculations are used to investigate the structure sensitivity of ethylene glycol (EG) decomposition on terraced and stepped platinum surfaces, including Pt(111) and Pt(211). On both surfaces, the binding energies of lightly dehydrogenated intermediates resulting from C−H bond scission in EG are typically stronger than the binding energies of intermediates associated with O−H bond breaking, and the corresponding kinetic trends generally track the thermochemical results. C−C and C−O bond cleavage have significantly higher barriers than dehydrogenation until relatively late in the dehydrogenation reaction network, and the transition state energies associated with C−C bond scission decrease almost monotonically with increasing levels of EG dehydrogenation, whereas the transition state energies of C−O bond breaking first decrease and then increase slightly. The most favorable reaction pathways for EG decomposition on Pt(111) and Pt(211) are very similar, with CO and H_2 as the main predicted products. However, Pt(211) shows substantially stronger binding of intermediates than does Pt(111). These results imply that platinum catalysts for EG conversion are likely to be relatively structure-sensitive in terms of activity but less sensitive in terms of selectivity. The results also demonstrate that linear relationships for prediction of both binding energies of dehydrogenated intermediates and barriers of elementary steps, which have been previously derived on close-packed terraces, are also found on steps, providing an important extension of these scaling and correlation principles to defected geometries. These relationships could, in turn, be used to accelerate the computational analysis of related complex reaction networks on undercoordinated surface features.

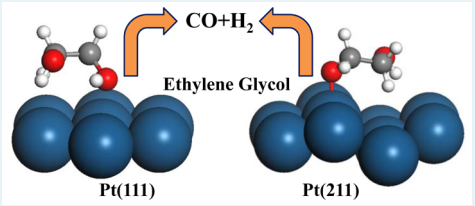

KEYWORDS: *ethylene glycol, structure sensitivity, platinum, density functional theory, biomass conversion*

1. INTRODUCTION

Catalytic conversion of renewable biomass feedstocks to a variety of useful fuels and value-added chemicals is attracting considerable interest because of its potential to reduce societal dependence on fossil fuels.[1−5] Generally, biomass derivatives have high levels of oxygen, and efficient deoxygenation chemistries are therefore necessary to transform the derivatives to useful chemical feedstocks.[6−9] A complementary chemistry involves aqueous phase reforming (APR) of biomass-derived oxygenates, such as polyols,[10−15] to produce hydrogen or syngas; the latter could be further combined with Fischer−Tropsch synthesis[16] to yield liquid alkanes. APR includes dehydrogenation, C−C bond scission, and the water−gas shift reaction.[12] To obtain the highest hydrogen selectivity, it is desirable to maximize dehydrogenation and C−C bond scission while minimizing C−O bond breaking.

The conversion of biomass-derived polyols, such as ethylene glycol (EG),[17−20] glycerol,[21−26] and sorbitol,[27−29] has been studied on a variety of catalysts. As the simplest polyol with a C/O stoichiometry of 1:1, EG can be produced from cellulose.[30−33] Investigations of EG conversion are of interest not only to enhance practical goals of hydrogen and syngas production, but also to provide fundamental insights into the underlying competition among C−H, O−H, C−C, and C−O bond cleavage in polyols. Such insights are, in turn, needed to understand activity and selectivity patterns in these complex chemistries. Given these motivating factors, the conversion of EG has been extensively studied on supported metal nanoparticles and on single crystal surfaces.[18,34−40] This work has demonstrated that platinum is an effective catalyst for aqueous phase reforming of EG because of its combination of high dehydrogenation activity and high selectivity to C−C bond breaking.[40] Results from ultrahigh vacuum experiments, density functional theory (DFT) calculations, and kinetic modeling[18−20] indicate that the decomposition pathway of EG on Pt(111) proceeds first through dehydrogenation and then via C−C bond scission of highly dehydrogenated intermediates. The selectivity to C−O bond scission, on the other hand, is relatively low, and the activity and selectivity of EG decomposition can be improved on Pt-based bimetallic catalysts.[12,39,41]

Although important progress has been made in understanding ethylene glycol chemistry on idealized metal surfaces, the impact of defects sites, such as steps, edges, and kinks, on these processes has received little attention. Such defect sites have different geometric and electronic properties, giving rise to

Received: November 30, 2014
Revised: February 18, 2015
Published: March 11, 2015

DOI: 10.1021/cs5019088
ACS Catal. 2015, 5, 2623−2631

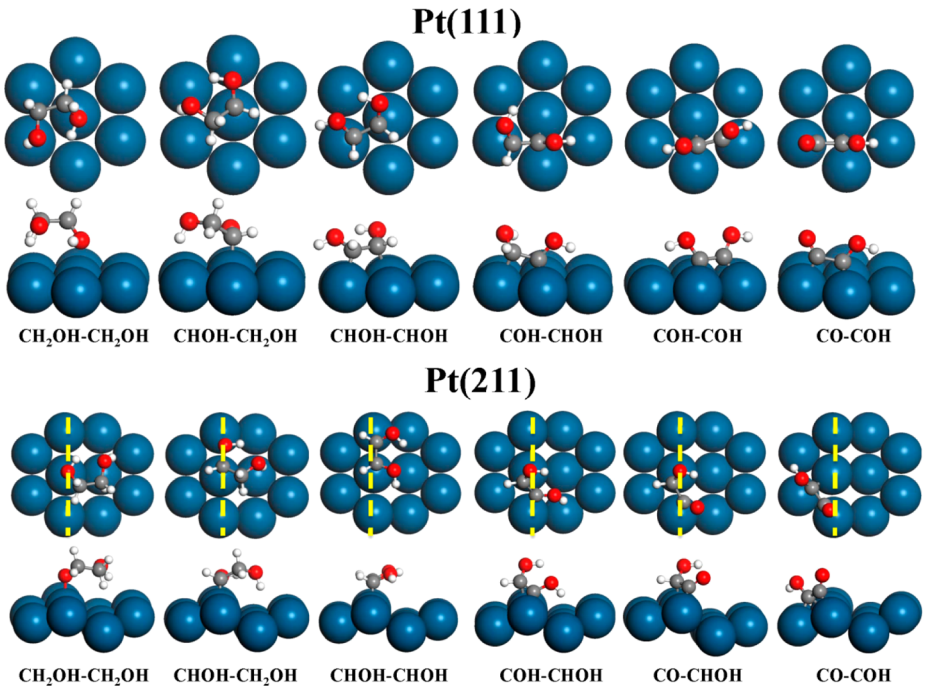

Figure 1. Optimized geometries of the most stable intermediates, at each level of dehydrogenation, involved in ethylene glycol dehydrogenation on Pt(111) and Pt(211). The blue, gray, red, and white spheres represent Pt, C, O, and H atoms, respectively. The dashed yellow line represents the step of Pt(211).

structure sensitivity wherein different catalytic activities and selectivities are manifested,[42−45] and to the best of our knowledge, the effects of structure sensitivity on polyol transformation at the molecular level have not been fully elucidated.

The goal of the present work is to provide insight into the above effects using EG decomposition as a model chemistry. The analysis is focused on EG chemistry on Pt(211) steps. Although EG decomposition on Pt(111) has been previously reported using a combination of DFT calculations and Brønsted−Evans−Polanyi (BEP) relationships,[18,20] we additionally summarize our own values of binding energies and barriers to provide fully consistent comparisons to the data reported on Pt(211). The (211) steps are clearly less thermodynamically stable than the Pt(111) surface, but they nonetheless represent reasonable models for general defects on Pt surfaces and Pt nanoparticles. For the thermodynamic and kinetic analysis, we focus on the reactants and intermediates determined by following the lowest barriers, as determined by full DFT calculations, at each stage in the EG decomposition pathway. In addition to being computationally efficient, this strategy is shown, by comparison to BEP-determined results for all possible elementary reaction steps, to be consistent with the most energetically favorable reaction pathways in the EG reaction network. We close by presenting general scaling and BEP relationships that may be used to efficiently map out energetic landscapes for EG decomposition and related classes of polyol chemistries on stepped platinum surfaces; to our knowledge, this is the first example of extension of scaling relationships for complex polyols to undercoordinated surfaces.

2. COMPUTATIONAL METHODS

Periodic DFT calculations were performed with the Vienna ab initio Simulation Package (VASP).[46,47] The exchange-correlation interaction is described by the generalized gradient approximation (GGA) and the Perdew−Wang 91 (PW91) functional.[48] The Kohn−Sham equations are solved in a plane wave basis set with a kinetic energy cutoff of 340 eV. A more accurate cutoff of 400 eV was also tested, and binding energies and activation barriers were found to be converged to less than 0.01 eV. For Pt(111) and Pt(211) surfaces, four-layer slab models were employed, with a p(3 × 3) unit cell on the (111) surface and a three-atom wide step on the (211) surface. The optimized lattice constant of bulk Pt is 3.98 Å. A (4 × 4 × 1) k-point mesh was used to sample the surface Brillouin zone, and a 12 Å vacuum was introduced between the repeated slabs along the z-direction. Convergence of binding energies with respect to all electronic parameters was confirmed. During optimization, the bottom two layers of the slab were fixed, while the remaining atoms and adsorbates were relaxed until the residual forces were <0.02 eV/Å. The test calculations showed that the binding energies and barriers were converged to <0.01 eV when the top three layers were relaxed.

The binding energies of dehydrogenated intermediates are defined as follows:

$$\mathrm{BE} = E_{\mathrm{C_2H_xO_2}*} - E_{\mathrm{sub}} - E_{\mathrm{EG(g)}} + \frac{6-x}{2}E_{\mathrm{H_2(g)}} \quad (1)$$

$E_{\mathrm{C_2H_xO_2}*}$, E_{sub}, $E_{\mathrm{EG(g)}}$, and $E_{\mathrm{H_2(g)}}$ are the total energies of the optimized $C_2H_xO_2$/substrate system, the clean substrate, and EG and hydrogen in the gas phase, respectively. In this definition, the binding energy can be thought of as the energy required to split gas phase EG into $C_2H_xO_2(g)$ and a stoichiometrically appropriate amount of $H_2(g)$, followed by adsorption of $C_2H_xO_2(g)$ onto the substrate. The barriers of the elementary steps are calculated by the climbing-image nudged elastic band (CI-NEB) method,[49,50] and the transition states are confirmed to possess a single imaginary frequency. We note that various possible initial states were considered for barrier calculations, and only the lowest such barriers are

DOI: 10.1021/cs5019088
ACS Catal. 2015, 5, 2623−2631

reported here. The reaction energies of the elementary steps were calculated with respect to the infinitely separated adsorbed reactant and products.

3. RESULTS

3.1. Geometries and Binding Energies of Dehydrogenated Intermediates. The thermochemistry of dehydrogenated intermediates is an important starting point to understanding the competition among dehydrogenation, C−C, and C−O bond cleavage at each level of dehydrogenation in EG decomposition. In this section, we therefore describe the structures and associated thermochemistry of EG and dehydrogenated intermediates on both Pt(111) and Pt(211). The most energetically favorable geometries of the dehydrogenated intermediates are shown in Figure 1, and the calculated binding energies are listed in Table S1.

3.1.1. Ethylene Glycol. On Pt(111), EG binds to the top site via one O atom with intramolecular H-bond formation, and the calculated binding energy is −0.37 eV. We note that it has also been reported that EG can bind to the surface via two O atoms at two adjacent top sites.[18] However, our calculations indicate that this structure is less stable by 0.29 eV because there is no intramolecular hydrogen bond formation. EG adsorption on Pt(211) occurs through one O atom bound to the top site at the step edge with the other OH group pointing toward the terrace surface. The calculated binding energy is −0.66 eV.

3.1.2. Intermediates with One Hydrogen Atom Removed. Dehydrogenated intermediates of EG can be formed from either C−H or O−H bond scission. The resulting CHOH−CH_2OH and CH_2O−CH_2OH intermediates prefer to bind to top sites via C and O atoms, respectively. The calculated binding energies of CHOH−CH_2OH, the most strongly bound intermediate at this level of dehydrogenation, are −0.13 eV on Pt(111) and −0.54 eV on Pt(211). This result may be related to the stronger binding of C atoms as compared with O atoms on platinum and to the fact that an intramolecular hydrogen bond is still present in CHOH−CH_2OH.

3.1.3. Intermediates with Two Hydrogen Atoms Removed. CHOH−CHOH binds the most strongly of all the intermediates at this level of dehydrogenation of EG. The binding occurs through two C atoms at two adjacent top sites with intramolecular hydrogen bonding between the OH groups. The calculated binding energies are 0.06 eV on Pt(111) and −0.28 eV on Pt(211), which are slightly stronger than those of the isomer COH−CH_2OH.

3.1.4. Intermediates with Three Hydrogen Atoms Removed. At this level of dehydrogenation, the COH−CHOH intermediate is the most stable on both considered surfaces. It favors adsorption through one C atom at a bridge site with the other C atom located at a top site. The calculated binding energy of −0.16 eV on Pt(211) is significantly stronger than that of 0.31 eV on Pt(111).

3.1.5. Intermediates with Four Hydrogen Atoms Removed. On Pt(111), the binding energy of 0.67 eV for COH−COH is slightly stronger than that of 0.82 eV for CO−CHOH. COH−COH adsorbs via one C atom at a top site, with the other C atom at a more favorable bridge site, whereas CO−CHOH adsorbs C atoms at two adjacent top sites. Conversely, the binding energy of 0.51 eV for COH−COH on Pt(211) is slightly weaker than that of 0.46 eV for CO−CHOH.

3.1.6. Intermediates with Five Hydrogen Atoms Removed. The most stable intermediate at this level of dehydrogenation, CO−COH, adsorbs via the CO group at a top site and the COH group at a bridge site on both surfaces; this configuration is slightly more stable than that with both groups adsorbed at adjacent top sites. The calculated binding energies are comparable on the two surfaces, with values of 0.99 and 0.94 eV on Pt(111) and Pt(211), respectively.

3.1.7. Intermediates with Six Hydrogen Atoms Removed. The most highly dehydrogenated species that could result from EG decomposition, CO−CO, binds to two adjacent top sites via its two C atoms on Pt(111), and the binding energy is 1.55 eV. CO−CO on Pt(211) is not stable and spontaneously dissociates.

Two overall trends emerge from the thermochemical results. First, dehydrogenated intermediates produced via C−H bond cleavage are generally more stable than those produced via O−H bond cleavage. Second, the binding energies of all dehydrogenated intermediates on stepped Pt(211) are stronger than those on Pt(111). This difference in binding strengths on the two surfaces could influence the activity or selectivity of EG conversion, as discussed further below.

3.2. Reaction Barriers for Decomposition of Dehydrogenated Intermediates. The decomposition of EG can produce 20 dehydrogenated intermediates, with close to 100 possible decomposition pathways. Explicit DFT-based transition state searches for all of these pathways would be computationally prohibitive, but much of the information associated with such an exhaustive search can be obtained by a very simple analysis that involves following the lowest dehydrogenation barriers at each level of dehydrogenation (in cases where competing pathways have very similar barriers, the pathway with the most favorable thermodynamics is considered for further analysis, as discussed in more detail below). The corresponding calculated barriers and reaction energies of elementary steps on Pt(111) and Pt(211) are listed in Table S2, and a brief comparison of the predictions of this approach and an alternative strategy relying on BEP relationships is provided in section 4.2.

3.2.1. Ethylene Glycol. For EG dehydrogenation on Pt(111), the calculated barrier of C−H bond breaking is 0.76 eV, with a reaction energy of −0.25 eV. This reaction is both thermodynamically and kinetically more favorable than O−H bond breaking, with barriers and reaction energies of 1.0 and 0.64 eV, respectively. This result is consistent with results reported by Kandoi et al.[20] and with the dehydrogenation sequence of similar polyols, such as glycerol, on Pt(111).[23] Similarly, C−H bond scission is more favorable than O−H bond scission for EG dehydrogenation on Pt(211). A barrier of 0.73 eV for C−H bond breaking is comparable to that on Pt(111), whereas this reaction is more exothermic on Pt(211), with a reaction energy of −0.51 eV. C−C and C−O bond cleavage on both surfaces is considerably more difficult than dehydrogenation, with energy barriers of more than 2.0 eV. Given these energetic considerations, CHOH−CH_2OH is the most favorable intermediate resulting from initial decomposition of EG on both Pt(111) and Pt(211).

3.2.2. Decomposition of Intermediates with One Hydrogen Atom Removed. There are seven elementary steps that could be involved in the decomposition of CHOH−CH_2OH. On Pt(111), CHOH−CHOH formation, with a barrier of 0.86 eV and reaction energy of −0.29 eV, is slightly more favorable than COH−CH_2OH formation, with a barrier of 0.95 eV and reaction energy of −0.19 eV. Although the barrier of CHOH−CH_2O formation (0.87 eV) from O−H bond breaking is comparable to that of CHOH−CHOH formation, the

DOI: 10.1021/cs5019088
ACS Catal. 2015, 5, 2623−2631

thermodynamics of O−H bond scission are significantly less favorable and are endothermic by 0.46 eV; we therefore select the C−H scission pathway for further analysis, which should be the dominant route if these elementary steps are at least partially reversible. The barriers of all other elementary steps on Pt(111) are >1.08 eV. On Pt(211), C−H bond scission is kinetically preferable to O−H, C−C, and C−O bond cleavage, and CHOH−CHOH formation has the lowest barrier and favorable thermodynamics. We note, in passing, that, although C−C and C−O bond breaking are not the kinetically favored steps at this level of dehydrogenation, the barriers of these steps are considerably lower than the corresponding barriers for EG itself. This result may stem, in part, from the proximity of the C−O bond to the surface on Pt(211) (Figure 1).

3.2.3. Decomposition of Intermediates with Two Hydrogen Atoms Removed. For decomposition of CHOH−CHOH, the barrier of 0.85 eV for C−H bond scission to COH−CHOH is comparable to that of 0.80 eV for O−H bond scission on Pt(111). However, the thermodynamics of C−H bond breaking is much more favorable (by 0.59 eV) than that of O−H bond breaking, and as discussed in section 3.2.2, we therefore choose this pathway for further analysis. C−H bond breaking has considerably lower barriers than do C−C and C−O bond cleavage. On Pt(211), C−H bond breaking, with a barrier of 0.22 eV, is facile and is much more favorable than O−H bond breaking. This barrier is also lower, by 0.63 eV, than that on Pt(111). Again, C−C and C−O bond cleavage in CHOH−CHOH have considerably higher barriers than the dehydrogenation reactions.

3.2.4. Decomposition of Intermediates with Three Hydrogen Atoms Removed. The decomposition of the COH−CHOH intermediate on Pt(111) could involve up to six elementary steps, including one C−H bond breaking and two O−H bond cleavage reactions. The barrier to break the O−H bond in the −COH group is 0.64 eV, which is lower by 0.24 eV than the barrier to C−H bond scission and lower by 0.49 eV than that of O−H bond scission in the −CHOH group. The lower barrier for O−H scission, in this case, is likely related to the production of a terminal CO group in the product molecule, CO−CHOH, which is known to bind very strongly to platinum surfaces. A similar trend is found on the (211) surface, where the barrier of O−H bond scission in the −COH group, 0.66 eV, is lower by 0.52 eV than that of C−H bond scission. In addition, the dehydrogenation processes are more facile compared with C−C and C−O bond cleavage on both surfaces.

3.2.5. Decomposition of Intermediates with Four Hydrogen Atoms Removed. The calculated barriers of C−H and O−H bond scission in CO−CHOH on Pt(111) are identical, with values of 0.80 eV, but the C−H bond breaking is exothermic, whereas O−H bond breaking is endothermic (Table S2). On Pt(211), the barrier of C−H bond breaking is 0.78 eV, which is lower by 0.40 eV than that of O−H bond breaking. Given these energetic values and following the arguments described in previous sections, we conclude that CO−COH formation via C−H bond scission is the more energetically favorable dehydrogenation process on the two surfaces. However, for this highly dehydrogenated intermediate, C−C bond scission has even lower barriers than dehydrogenation, with values of 0.47 eV on Pt(111) and 0.45 eV on Pt(211). Furthermore, C−C bond breaking is highly exothermic, by 0.72 and 1.23 eV on Pt(111) and Pt(211), respectively, and C−O bond breaking barriers are significantly higher than are C−C scission barriers on both surfaces. The favorable kinetics and thermochemistry of C−C bond activation in this intermediate reflect the strong binding of CO to platinum surfaces.

3.2.6. Decomposition of Intermediates with Five Hydrogen Atoms Removed. Although the CO−CHOH intermediate may undergo C−C bond scission, as discussed in section 3.2.5 above, it is nonetheless instructive, for the sake of completeness, to consider further dehydrogenation and C−C/C−O activation in the resulting intermediates. The dehydrogenation of the CO−COH intermediate via O−H bond breaking is slightly endothermic, by 0.06 eV, with a barrier of 0.61 eV on Pt(111); interestingly, this process is exothermic by 0.30 eV, with a barrier of 0.85 eV, on Pt(211). The barrier of C−C bond scission is slightly higher (0.72 eV) than that of dehydrogenation, but it is highly exothermic by 0.96 eV on Pt(111), suggesting that these two processes might have comparable rates. On Pt(211), C−C bond scission is both thermodynamically and kinetically more facile than dehydrogenation. Finally, the process of C−O bond breaking has considerably higher barriers on both Pt(111) and Pt(211) (Table S2).

3.2.7. Decomposition of Intermediates with Six Hydrogen Atoms Removed. The CO−CO intermediate that could be formed from CO−COH dehydrogenation can undergo facile C−C bond activation with a barrier of 0.05 eV on Pt(111), leaving two CO molecules on the surface. As mentioned above, CO−CO is not stable on Pt(211) and spontaneously dissociates.

3.3. Free Energy Diagrams. On the basis of the thermochemical and kinetic results in sections 3.1 and 3.2, Gibbs free energy diagrams for EG decomposition on Pt(111) and Pt(211) are constructed and plotted in Figures 2 and 3, respectively. The free energies are determined by taking into account the entropy contributions of EG adsorption and H_2

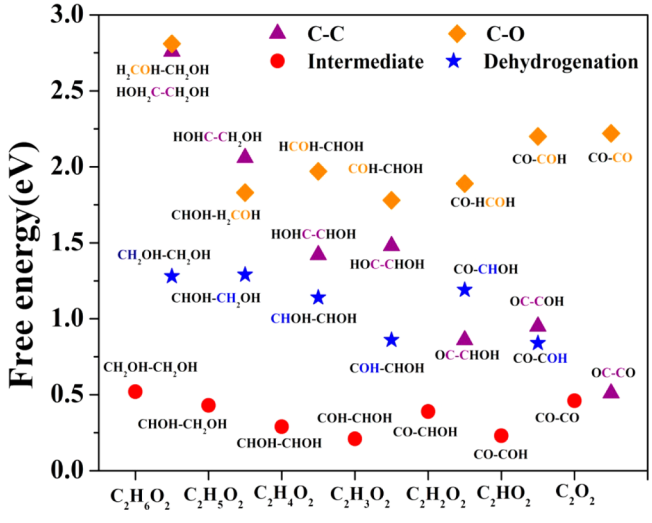

Figure 2. Free energy diagram of ethylene glycol decomposition on Pt(111) at 500 K and standard pressures. Red points represent the adsorption thermodynamics of the dehydrogenated intermediates with respect to the clean surface and ethylene glycol and H_2 in gas phase. Blue stars, purple triangles, and orange diamonds represent transition states associated with the lowest-barrier pathways for dehydrogenation, C−C, and C−O bond breaking, respectively, for each step in the dehydrogenation network (see section 3.2 in the text for additional details). The blue, purple, and orange letters indicate the bonds that are broken.

DOI: 10.1021/cs5019088
ACS Catal. 2015, 5, 2623−2631

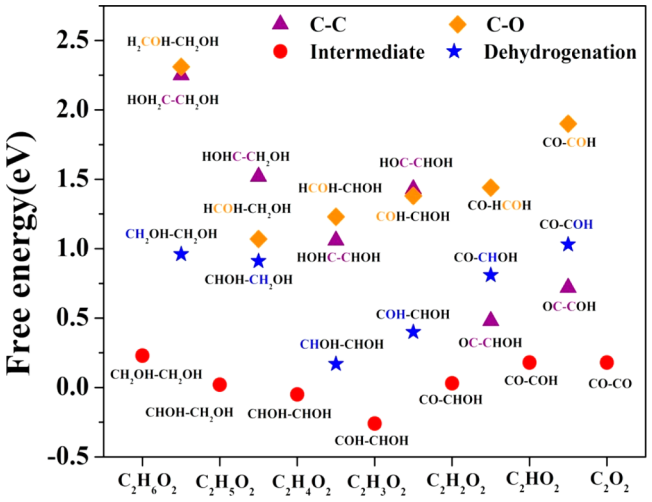

Figure 3. Free energy diagram of ethylene glycol decomposition on Pt(211) at 500 K and standard pressures. The symbols have the same meanings as described in the caption of Figure 2

desorption. We assume that the most important such contributions are from the translational entropy, calculated as

$$S = 1.5R \ln(2\pi MkT) - 3R \ln h + R \ln(kT/P) + 2.5R \quad (2)$$

where M, R, k, h, T, and P are the molecular weight, ideal gas constant, Boltzmann constant, Planck constant, temperature, and pressure, respectively. In these free energy diagrams, the free energies of the intermediates are reported at 500 K and standard pressures, which are typical conditions for aqueous phase reforming reactions of polyols in biomass conversion. At these conditions, we estimate that EG in the gas phase loses about 0.89 eV of entropic energy (TS) when adsorbing, and H_2 correspondingly gains 0.66 eV when desorbing into the gas phase. The reference state corresponds to the clean surface and to EG and H_2 in the gas phase. We note that similar approaches have been successfully used to determine free energy changes for use in microkinetic modeling for a variety of heterogeneous catalytic reactions.[51,52]

From the free energy diagrams on the two surfaces, it is clearly seen that EG dehydrogenation processes are initially exothermic and then become endothermic. For the lightly dehydrogenated intermediates (before approximately CO−CHOH), the dehydrogenation steps are more facile than are C−C and C−O bond cleavage. However, C−C bond breaking becomes more favorable for the decomposition of highly dehydrogenated intermediates. Moreover, the transition state energies of C−C bond cleavage decrease almost monotonically with increasing levels of dehydrogenation, whereas for C−O bond breaking, the transition state energies drop significantly from EG to CHOH−CH_2OH and then increase gradually with additional dehydrogenation. A similar bond-breaking sequence has been found in glycerol decomposition on Pt(111).[23−25]

We note that the intermediates analyzed on both platinum surfaces, determined by the kinetic procedure described in section 3.2, correspond very closely to the most thermodynamically stable intermediates at each level of dehydrogenation. On Pt(211), in fact, the intermediates are identical (Table S1), whereas on Pt(111), the only difference is seen after removal of four hydrogen atoms from EG, in which the analyzed intermediate from the kinetic pathway analysis is CO−CHOH and the most thermodynamically stable intermediate is COH−COH. As discussed further below, these minor differences do not, in any way, affect the comparisons of structure sensitivity that are the major focus of this paper. We further note that the results in Figure 2 compare favorably with the results of Kandoi et al.;[20] modest differences arise from different numbers of layers in the two analyses and from the use of full NEB transition state searches in the present work, as opposed to BEP analyses in the cited reference.

3.4. Reaction Pathways of Ethylene Glycol Decomposition. The reaction pathways for EG decomposition on Pt(111) and Pt(211) at 500 K and standard pressures, derived from the thermochemical and kinetic results in Figures 2 and 3, are summarized in Figure 4. As is discussed further below, these

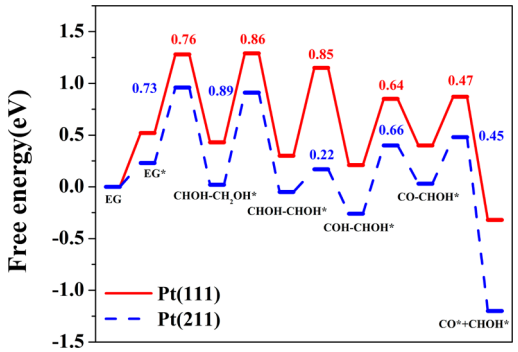

Figure 4. Reaction pathways of ethylene glycol decomposition on Pt(111) and Pt(211) at 500 K and standard pressures.

diagrams provide important qualitative and semiquantitative insights into the preferred reaction pathways for EG decomposition on these surfaces. Although a full microkinetic model of the intermediates and elementary reaction steps could provide quantitative estimates of selectivities and reaction pathways, it has been found previously that free energy and microkinetic analyses often provide similar conclusions,[20] we adopt the former approach in the following.

In general, it is seen that the reaction pathways on the two surfaces are the same, first involving dehydrogenation of EG to CO−CHOH, followed by cleavage of the C−C bond of CO−CHOH to form CO and CHOH. CHOH can, in turn, decompose to adsorbed CO and hydrogen, as described in previous studies.[53−56] Hence, the primary products from decomposition of EG on both surfaces will be CO and H_2. We note, however, that competing pathways involving C−O bond activation (particularly in an intermediate early in the reaction network; Figures 2 and 3) are relatively more favorable on Pt(211) than on Pt(111). Although we do not predict that these are the most energetically preferred pathways, the results nonetheless suggest that secondary products resulting from C−O bond activation are likely to be more common on the stepped surfaces.

The barriers for dehydrogenation and C−C bond breaking are generally comparable on the two surfaces, with the exception of the dehydrogenation of CHOH−COH, which has a significantly lower barrier on Pt(211) than on Pt(111). In contrast, the decomposition of EG on Pt(211) is considerably more exothermic than on Pt(111) as a result of the stronger binding of intermediates on Pt(211). This stronger binding implies that effective activation barriers on the stepped surfaces will be lower than the corresponding barriers on terraces. However, the stronger binding of product CO on the stepped

DOI: 10.1021/cs5019088
ACS Catal. 2015, 5, 2623−2631

surfaces could also lead to increased poisoning of the steps and to a consequent decrease in activity. In decomposition of EG at a gas−solid interface, poisoning would most likely be the dominant effect, and steps would therefore exhibit lower activity for EG conversion. In the liquid phase, however, CO can be removed by water gas shift reaction (WGSR) chemistry, thus reducing the poisoning effect. Since APR chemistry is typically carried out at pressures of ∼30 bar, water can remain liquid, even at temperatures as high as 500 K. Our DFT model is thus relevant to aqueous phase conditions, and although the model does not explicitly include the effects of hydrogen bonding from solvent water molecules, we expect that such effects will be similar on the Pt(111) and Pt(211) surfaces and will not alter the reactivity trends. Although the removal of CO by WGS is difficult to quantify, there is some evidence to suggest that the WGSR rate on Pt(211) is higher than that on Pt(111) with water at high pressures.[57] If the mitigation of CO poisoning on steps through the WGSR is sufficiently high, then when combined with the enhanced step binding described above, higher activity on the steps would result.

We note that, to support the above theoretical analyses, it would be extremely helpful to have additional single crystal experiments on Pt(111) and Pt(211).[18,26] In addition, experiments on size-selected platinum nanoparticles under realistic APR conditions could be of benefit. On smaller nanoparticles, there will be a larger fraction of edge and defect sites present; so the chemistry of such particles may be closer to that predicted on the Pt(211) surfaces.

4. DISCUSSION

As described above, the decomposition of EG involves a very complex reaction network, including 20 dehydrogenated intermediates and more than 100 elementary steps. Although important insights into the reaction chemistry can be obtained using the approaches described in section 3, it is also of interest to explore accelerated strategies for probing the thermochemistry and kinetics of the various intermediates. Such approaches have been introduced previously on planar transition metal surfaces,[23−25,58] and below, we demonstrate that they are also effective on Pt(211) steps.

4.1. Scaling relationship for binding energy prediction. A scaling relationship for binding energy estimation can be motivated by simple bond order conservation principles. This approach has previously been used to describe the adsorption of a large ensemble of intermediates from glycerol, ethylene glycol, and ethanol dehydrogenation on Pt(111).[23−25] The estimated binding energies of the dehydrogenated intermediates are calculated using the following expression:

$$\mathrm{BE}_{\mathrm{C_2H_xO_2}*} = \sum_i p_{\mathrm{C}_i} \nu_{\mathrm{C}_i} + \sum_i p_{\mathrm{O}_i} \nu_{\mathrm{O}_i} + \sum_i p_{\mathrm{C}_i\mathrm{O}_i} \nu_{\mathrm{C}_i} \nu_{\mathrm{O}_i} + \mathrm{BE}_{\mathrm{EG}*} \quad (3)$$

where

$$\nu_i = \frac{n_{\mathrm{max},i} - n_{\mathrm{bond},i}}{n_{\mathrm{max},i}} \quad (4)$$

In this definition, $\mathrm{BE}_{\mathrm{C_2H_xO_2}*}$ is the binding energy of the adsorbed $C_2H_xO_2$ intermediate with respect to gas phase EG, the appropriate clean surface, and a stoichiometrically appropriate amount of gas phase H_2 molecules, and $\mathrm{BE}_{\mathrm{EG}*}$ is the binding energy of EG with respect to the appropriate clean surface and EG in gas phase. x is dependent on the level of dehydrogenation, ranging from 0 to 6. $\nu_{\mathrm{C}i}$ and $\nu_{\mathrm{O}i}$ are used to measure the degree of undersaturation of the C and O atoms, as described in eq 4, where $n_{\mathrm{max},i}$ is the maximum number bonds that the atom can form (4 and 2 for C and O, respectively) and $n_{\mathrm{bond},i}$ is the actual number of atoms bonded to C/O in the intermediates. $p_{\mathrm{C}i}$, $p_{\mathrm{O}i}$, and $p_{\mathrm{CiO}i}$ are fitting parameters determined by comparison with the explicitly calculated DFT binding energies. To obtain a satisfactory fit, the first two terms in eq 3 are over all C and O atoms, but it is only necessary for the third term to treat nearest-neighbor C−O pairs (inclusion of C−C pairs does not significantly affect the fit). In addition, the parameters for the two C/O atoms are the same because of the symmetry of the EG molecule.

The predicted binding energies of EG dehydrogenated intermediates using this correlation scheme are listed in Table S1, and a comparison of predicted binding energies with those from DFT calculations on Pt(111) and Pt(211) is shown in Figure 5. Compared with the binding energies determined from

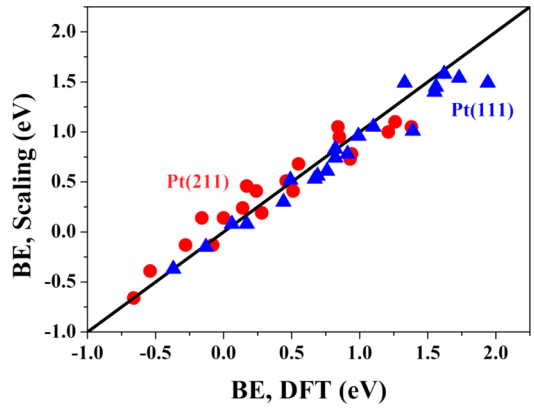

Figure 5. Comparison of predicted binding energies of EG dehydrogenated intermediates with binding energies from explicit DFT calculations on Pt(111) and Pt(211), denoted as blue triangles and red points, respectively.

DFT calculations, the standard errors are 0.12 eV on Pt(111) and 0.15 eV on Pt(211), which are within the generally accepted accuracy of DFT calculations. On Pt(111), the fitting parameters of p_{C1}, p_{O1}, and p_{C1O1} are 0.90, 1.95, and −2.16, respectively. On Pt(211), these parameters become 1.07, 1.61, and −1.73, respectively. The differences between the parameter values on Pt(111) and Pt(211) are relatively small and likely result, in part, from the different bond strengths of atomic C and O on the two surfaces. The calculated binding energy of atomic C on Pt(111) is stronger by 0.14 eV than that on Pt(211); However, the binding energy of atomic O on Pt(111) is weaker by 0.26 eV. This simple comparison hints that the binding energies of C-containing intermediates on steps will be weaker than the corresponding values on terraces, and the binding energies of O-containing intermediates on steps will be stronger than those on terraces. Since, according to eq 3, more positive energies indicate weaker binding, the parameter p_{C1} on Pt(211) should be larger than the value of this parameter on Pt(111). However, the parameter p_{O1} on Pt(211) should be smaller than the corresponding value on Pt(111), and these are exactly the trends that result from detailed fitting to DFT-determined binding energies. We note, in passing, that the fitting parameters on Pt(111) are the same as those previously determined in the binding energy predictions for glycerol

DOI: 10.1021/cs5019088
ACS Catal. 2015, 5, 2623−2631

dehydrogenated intermediates on Pt(111).[23,24] In like manner, we expect that the Pt(211) parameters determined for EG will be transferrable to other polyols, indicating that this correlation scheme is powerful and transferable for binding energy estimation of a variety of intermediates derived from polyol dehydrogenation.

4.2. BEP Relationships for Barrier Prediction. On the basis of the calculated kinetics and thermodynamics of the elementary steps involved in the decomposition of EG (Table S2), BEP relationships[59−63] for EG decomposition on Pt(111) and Pt(211) are developed. The elementary steps are written in the exothermic direction for the surface-adsorbed reactants and products, and transition state (E_{TS}) and final state (E_{FS}) energies are referenced to the gas phase reactants in each elementary step. From Figures 6 and 7, it is seen that there do

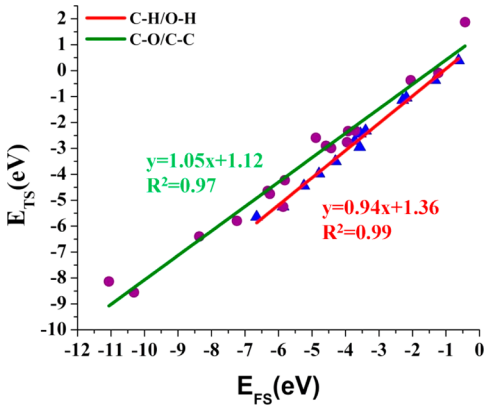

Figure 6. BEP relationship for C−H/O−H and C−C/C−O bond breaking on Pt(111). The transition state (E_{TS}) and final state (E_{FS}) energies are referenced to the initial state in the gas phase, and the reactions are written in the exothermic direction.

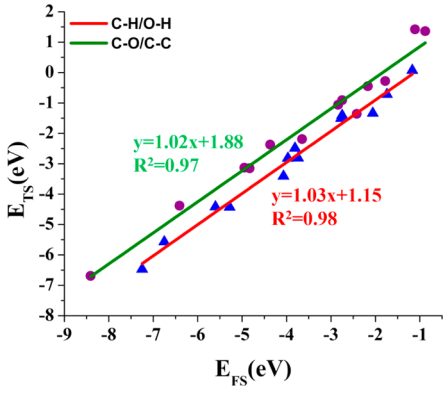

Figure 7. BEP relationship for C−H/O−H and C−C/C−O bond breaking on Pt(211). The transition state (E_{TS}) and final state (E_{FS}) energies are referenced to the initial state in the gas phase, and the reactions are written in the exothermic direction.

exist linear relationships between E_{TS} and E_{FS}. The relationships for C−C/C−O bond breaking and for dehydrogenation on Pt(111) are $E_{TS} = 1.05E_{FS} + 1.12$ and $E_{TS} = 0.94E_{FS} + 1.36$, and the corresponding relationships on Pt(211) are $E_{TS} = 1.02E_{FS} + 1.88$ and $E_{TS} = 1.03E_{FS} + 1.15$. The standard errors for dehydrogenation, C−C, and C−O bond breaking on Pt(111) are 0.10, 0.27, and 0.12 eV, and the corresponding values are 0.15, 0.13, and 0.18 eV on Pt(211).

It is seen that the slopes are similar on Pt(111) and Pt(211), and the intercepts vary in a more complex manner between the two surfaces. We note that, even with similar slopes of the BEP relationships (defined above), differences in actual activation barriers between the (211) and (111) surfaces are not solely determined by the difference in BEP intercepts, and the barriers may thus be either larger or smaller on steps vs terraces, depending upon the exothermicity of the surface reaction and the strength of reactant binding to the surface.

Finally, for purposes of comparison, and as mentioned briefly in section 3, we note that another type of free energy diagram on Pt(111) and Pt(211) can be plotted using the energies of the most stable dehydrogenated intermediates, as well as the lowest transition state energies for dehydrogenation, C−C, and C−O bond breaking (as determined using BEP relationships) at each level of dehydrogenation, as shown in Figure S1 and S2, respectively. This type of free energy diagram assumes that the scrambling between dehydrogenated intermediates at the same level of dehydrogenation is rapid. As shown in Figures S1 and S2, the intermediates and transition states identified by this alternate approach are very similar to those found by following the lowest barriers in the reaction network, as described in section 3, and the trends and mechanistic conclusions are identical between the two strategies. These similarities imply that the mechanistic conclusions derived above are not too sensitive to the particular kinetic model that is applied to the DFT data and that these conclusions provide a reasonable description of EG chemistry on Pt(111) and Pt(211).

5. CONCLUSIONS

The decomposition of the simplest biomass-derived polyol, ethylene glycol, is analyzed with periodic DFT calculations on Pt(111) and Pt(211). On both surfaces, it is found that, at early stages in the dehydrogenation reaction network, intermediates produced via C−H bond scission are more stable than those produced from O−H bond scission. In addition, the elementary dehydrogenation reactions are exothermic early in the dehydrogenation network, and then they become endothermic after several hydrogen atoms have been removed. Cleavage of C−C and C−O bonds in EG itself has very high barriers, but the barrier of C−C bond scission decreases almost monotonically with successive EG dehydrogenation, and it ultimately becomes lower than the corresponding dehydrogenation barriers. The barriers of C−O bond scission, in contrast, first decrease and then increase as successive hydrogen atoms are removed from EG. The net result of these competing energetic trends is that dehydrogenation is favorable on both surfaces early in the reaction network, and C−C activation subsequently becomes favorable after a significant amount of dehydrogenation has occurred. These trends further suggest that CO and H_2 will be the dominant products formed on both Pt(111) and Pt(211), implying that the reaction selectivity is not highly structure sensitive, even though a modestly larger amount of minority C−O scission products might be formed on Pt(211). Nearly all intermediates bind more strongly to Pt(211) than to Pt(111), however, leading to lower effective activation barriers on the stepped surface. If CO poisoning on Pt(211) is mitigated by the water−gas shift reaction in the liquid phase, then this difference in effective barriers will result in higher activity on stepped surfaces. Finally, it is shown that linear correlations for binding energies of dehydrogenated intermediates and the barriers of elementary steps, which have previously been developed on close-packed (111) surfaces, also

DOI: 10.1021/cs5019088
ACS Catal. 2015, 5, 2623−2631

hold on Pt(211) stepped surfaces. Such correlations open new possibilities for rapid and efficient analysis of polyol-based reaction networks on undercoordinated transition metal surfaces.

■ ASSOCIATED CONTENT

Supporting Information

The following file is available free of charge on the ACS Publications website at DOI: 10.1021/cs5019088.

Binding energies of dehydrogenated intermediates, barriers and reaction energies of key elementary steps, and additional free energy diagrams (PDF)

■ AUTHOR INFORMATION

Corresponding Author

*E-mail: jgreeley@purdue.edu.

Notes

The authors declare no competing financial interest.

■ ACKNOWLEDGMENTS

This work is supported as part of the Institute for Atom-efficient Chemical Transformations (IACT), an Energy Frontier Research Center funded by the U.S. Depart of Energy, Office of Science, Office of Basic Energy Sciences. J.G. acknowledges an Early Career Award from the Department of Energy, Office of Science, Office of Basic Energy Sciences, Chemical Sciences, Geosciences, and Biosciences Division. Use of the Center for Nanoscale Materials was supported by the U.S. Department of Energy, Office of Science, Office of Basic Energy Sciences, under Contract No. DE-AC02-06CH11357. Computational resources provided by the National Energy Research Scientific Computing Center (NERSC) are gratefully acknowledged.

■ REFERENCES

(1) Cortright, R. D.; Davda, R. R.; Dumesic, J. A. *Nature* **2002**, *418*, 964.
(2) Kunkes, E. L.; Simonetti, D. A.; West, R. M.; Serrano-Ruiz, J. C.; Gartner, C. A.; Dumesic, J. A. *Science* **2008**, *322*, 417.
(3) Huber, G. W.; Iborra, S.; Corma, A. *Chem. Rev.* **2006**, *106*, 4044.
(4) O'Neill, B. J.; Jackson, D. H. K.; Crisci, A. J.; Farberow, C. A.; Shi, F. Y.; Alba-Rubio, A. C.; Lu, J. L.; Dietrich, P. J.; Gu, X. K.; Marshall, C. L.; Stair, P. C.; Elam, J. W.; Miller, J. T.; Ribeiro, F. H.; Voyles, P. M.; Greeley, J.; Mavrikakis, M.; Scott, S. L.; Kuech, T. F.; Dumesic, J. A. *Angew. Chem., Int. Ed.* **2013**, *52*, 13808.
(5) Zhang, H. B.; Gu, X. K.; Canlas, C.; Kropf, A. J.; Aich, P.; Greeley, J. P.; Elam, J. W.; Meyers, R. J.; Dumesic, J. A.; Stair, P. C.; Marshall, C. L. *Angew. Chem., Int. Ed.* **2014**, *53*, 12132.
(6) Furimsky, E. *Appl. Catal., A* **2000**, *199*, 147.
(7) Wawrzetz, A.; Peng, B.; Hrabar, A.; Jentys, A.; Lemonidou, A. A.; Lercher, J. A. *J. Catal.* **2010**, *269*, 411.
(8) Peng, B. X.; Zhao, C.; Mejia-Centeno, I.; Fuentes, G. A.; Jentys, A.; Lercher, J. A. *Catal. Today* **2012**, *183*, 3.
(9) Choudhary, T. V.; Phillips, C. B. *Appl. Catal., A* **2011**, *397*, 1.
(10) Shabaker, J. W.; Huber, G. W.; Davda, R. R.; Cortright, R. D.; Dumesic, J. A. *Catal. Lett.* **2003**, *88*, 1.
(11) Shabaker, J. W.; Davda, R. R.; Huber, G. W.; Cortright, R. D.; Dumesic, J. A. *J. Catal.* **2003**, *215*, 344.
(12) Huber, G. W.; Shabaker, J. W.; Evans, S. T.; Dumesic, J. A. *Appl. Catal., B* **2006**, *62*, 226.
(13) Wen, G. D.; Xu, Y. P.; Ma, H. J.; Xu, Z. S.; Tian, Z. J. *Int. J. Hydrogen Energy* **2008**, *33*, 6657.
(14) Dietrich, P. J.; Wu, T. P.; Sumer, A.; Dumesic, J. A.; Jellinek, J.; Delgass, W. N.; Ribeiro, F. H.; Miller, J. T. *Top. Catal.* **2013**, *56*, 1814.
(15) Dietrich, P. J.; Lobo-Lapidus, R. J.; Wu, T. P.; Sumer, A.; Akatay, M. C.; Fingland, B. R.; Guo, N.; Dumesic, J. A.; Marshall, C. L.; Stach, E.; Jellinek, J.; Delgass, W. N.; Ribeiro, F. H.; Miller, J. T. *Top. Catal.* **2012**, *55*, 53.
(16) Khodakov, A. Y.; Chu, W.; Fongarland, P. *Chem. Rev.* **2007**, *107*, 1692.
(17) Yu, W. T.; Salciccioli, M.; Xiong, K.; Barteau, M. A.; Vlachos, D. G.; Chen, J. G. G. *ACS Catal.* **2014**, *4*, 1409.
(18) Salciccioli, M.; Yu, W. T.; Barteau, M. A.; Chen, J. G. G.; Vlachos, D. G. *J. Am. Chem. Soc.* **2011**, *133*, 7996.
(19) Salciccioli, M.; Vlachos, D. G. *ACS Catal.* **2011**, *1*, 1246.
(20) Kandoi, S.; Greeley, J.; Simonetti, D.; Shabaker, J.; Dumesic, J. A.; Mavrikakis, M. *J. Phys. Chem. C* **2011**, *115*, 961.
(21) Pagliaro, M.; Ciriminna, R.; Kimura, H.; Rossi, M.; Della Pina, C. *Angew. Chem., Int. Ed.* **2007**, *46*, 4434.
(22) Soares, R. R.; Simonetti, D. A.; Dumesic, J. A. *Angew. Chem., Int. Ed.* **2006**, *45*, 3982.
(23) Liu, B.; Greeley, J. *J. Phys. Chem. C* **2011**, *115*, 19702.
(24) Liu, B.; Greeley, J. *Top. Catal.* **2012**, *55*, 280.
(25) Liu, B.; Greeley, J. *Phys. Chem. Chem. Phys.* **2013**, *15*, 6475.
(26) Skoplyak, O.; Barteau, M. A.; Chen, J. G. *ChemSusChem* **2008**, *1*, 524.
(27) Li, N.; Huber, G. W. *J. Catal.* **2010**, *270*, 48.
(28) Kirilin, A. V.; Tokarev, A. V.; Murzina, E. V.; Kustov, L. M.; Mikkola, J. P.; Murzin, D. Y. *ChemSusChem* **2010**, *3*, 708.
(29) Kim, Y. T.; Dumesic, J. A.; Huber, G. W. *J. Catal.* **2013**, *304*, 72.
(30) Ji, N.; Zhang, T.; Zheng, M. Y.; Wang, A. Q.; Wang, H.; Wang, X. D.; Chen, J. G. G. *Angew. Chem., Int. Ed.* **2008**, *47*, 8510.
(31) Zheng, M. Y.; Wang, A. Q.; Ji, N.; Pang, J. F.; Wang, X. D.; Zhang, T. *ChemSusChem* **2010**, *3*, 63.
(32) Liu, Y.; Luo, C.; Liu, H. C. *Angew. Chem., Int. Ed.* **2012**, *51*, 3249.
(33) Wang, A. Q.; Zhang, T. *Acc. Chem. Res.* **2013**, *46*, 1377.
(34) Li, S. R.; Zhang, C. X.; Zhang, P.; Wu, G. W.; Ma, X. B.; Gong, J. L. *Phys. Chem. Chem. Phys.* **2012**, *14*, 4066.
(35) Griffin, M. B.; Jorgensen, E. L.; Medlin, J. W. *Surf. Sci.* **2010**, *604*, 1558.
(36) Skoplyak, O.; Barteau, M. A.; Chen, J. G. G. *Catal. Today* **2009**, *147*, 150.
(37) Skoplyak, O.; Menning, C. A.; Barteau, M. A.; Chen, J. G. G. *Top. Catal.* **2008**, *51*, 49.
(38) Skoplyak, O.; Barteau, M. A.; Chen, J. G. G. *Surf. Sci.* **2008**, *602*, 3578.
(39) Skoplyak, O.; Barteau, M. A.; Chen, J. G. G. *J. Phys. Chem. B* **2006**, *110*, 1686.
(40) Davda, R. R.; Shabaker, J. W.; Huber, G. W.; Cortright, R. D.; Dumesic, J. A. *Appl. Catal., B* **2003**, *43*, 13.
(41) Kim, H. D.; Park, H. J.; Kim, T. W.; Jeong, K. E.; Chae, H. J.; Jeong, S. Y.; Lee, C. H.; Kim, C. U. *Int. J. Hydrogen Energy* **2012**, *37*, 8310.
(42) Michalak, W. D.; Krier, J. M.; Komvopoulos, K.; Somorjai, G. A. *J. Phys. Chem. C* **2013**, *117*, 1809.
(43) Alayoglu, S.; Aliaga, C.; Sprung, C.; Somorjai, G. A. *Catal. Lett.* **2011**, *141*, 914.
(44) Hammer, B.; Nielsen, O. H.; Norskov, J. K. *Catal. Lett.* **1997**, *46*, 31.
(45) Pushkarev, V. V.; Musselwhite, N.; An, K.; Alayoglu, S.; Somorjai, G. A. *Nano Lett.* **2012**, *12*, 5196.
(46) Kresse, G.; Furthmuller, J. *Phys. Rev. B* **1996**, *54*, 11169.
(47) Kresse, G.; Furthmuller, J. *Comput. Mater. Sci.* **1996**, *6*, 15.
(48) Perdew, J. P.; Wang, Y. *Phys. Rev. B* **1992**, *45*, 13244.
(49) Henkelman, G.; Uberuaga, B. P.; Jonsson, H. *J. Chem. Phys.* **2000**, *113*, 9901.
(50) Henkelman, G.; Jonsson, H. *J. Chem. Phys.* **2000**, *113*, 9978.
(51) Gokhale, A. A.; Kandoi, S.; Greeley, J. P.; Mavrikakis, M.; Dumesic, J. A. *Chem. Eng. Sci.* **2004**, *59*, 4679.
(52) Kandoi, S.; Greeley, J.; Sanchez-Castillo, M. A.; Evans, S. T.; Gokhale, A. A.; Dumesic, J. A.; Mavrikakis, M. *Top. Catal.* **2006**, *37*, 17.

DOI: 10.1021/cs5019088
ACS Catal. 2015, 5, 2623−2631

(53) Greeley, J.; Mavrikakis, M. *J. Am. Chem. Soc.* **2004**, *126*, 3910.
(54) Desai, S. K.; Neurock, M.; Kourtakis, K. *J. Phys. Chem. B* **2002**, *106*, 2559.
(55) Kramer, Z. C.; Gu, X. K.; Zhou, D.; Li, W. X.; Skodje, R. T. *J. Phys. Chem. C* **2014**, *118*, 12364.
(56) Gu, X. K.; Qiao, B. T.; Huang, C. Q.; Ding, W. C.; Sun, K. J.; Zhan, E. S.; Zhang, T.; Liu, J. Y.; Li, W. X. *ACS Catal.* **2014**, *4*, 3886.
(57) Stamatakis, M.; Chen, Y.; Vlachos, D. G. *J. Phys. Chem. C* **2011**, *115*, 24750.
(58) Liu, B.; Cheng, L.; Curtiss, L.; Greeley, J. *Surf. Sci.* **2014**, *622*, 51.
(59) Alcala, R.; Mavrikakis, M.; Dumesic, J. A. *J. Catal.* **2003**, *218*, 178.
(60) Norskov, J. K.; Bligaard, T.; Logadottir, A.; Bahn, S.; Hansen, L. B.; Bollinger, M.; Bengaard, H.; Hammer, B.; Sljivancanin, Z.; Mavrikakis, M.; Xu, Y.; Dahl, S.; Jacobsen, C. J. H. *J. Catal.* **2002**, *209*, 275.
(61) Gu, X. K.; Li, W. X. *J. Phys. Chem. C* **2010**, *114*, 21539.
(62) Zaffran, J.; Michel, C.; Auneau, F.; Delbecq, F.; Sautet, P. *ACS Catal.* **2014**, *4*, 464.
(63) Loffreda, D.; Delbecq, F.; Vigne, F.; Sautet, P. *Angew. Chem., Int. Ed.* **2009**, *48*, 8978.

DOI: 10.1021/cs5019088
ACS Catal. 2015, 5, 2623−2631